SAE INTERNATIONAL

ARTICLE INFO
Article ID: 02-16-02-0010

doi:10.4271/02-16-02-0010

Influence of Yaw and Lateral Offset on the Aerodynamics of a Two-Truck Platoon

Johannes Törnell,[1] Simone Sebben,[1] and Per Elofsson[2]

[1]Chalmers Tekniska Högskola, Sweden
[2]Fluid Mechanics, Scania CV, Sweden

Abstract

Governmental regulations and customer demand for more energy-efficient vehicles are driving the development of new solutions in the automotive sector. One way of improving energy efficiency is by reducing the aerodynamic drag. A possible solution to achieve this is the concept of vehicles driving in close proximity, which is now becoming feasible considering the advances in vehicle automation and communication. This study focuses on the behavior of aerodynamic forces and flow effects in a two-truck platoon when more realistic road conditions, such as lateral offset and yaw, are present. The study is primarily numerical, but the results are validated against an experimental campaign conducted earlier by the authors. The main findings are that the drag of the leading truck is mostly governed by the base pressure of its trailer and that the truck sees only minor changes when a lateral offset is added, except at very short intervehicle distances. For larger yaw angles, the leading truck sees an increase in the effective yaw angle for the trailer, resulting in lower efficiency of the platoon. The behavior of the trailing truck is much more complex, with several different effects being observed when yaw and lateral offset are added. When yaw is added, the movement and increased intensity of the stagnation region adds to drag, while the change in effective yaw angle lowers the drag of the vehicle. This causes the benefit of platooning to vary with both yaw angle and vehicle distance. The addition of a lateral offset in the leeward direction can partially compensate for the negative effects of yaw on drag.

History

Received: 31 Mar 2022
Revised: 13 Jun 2022
Accepted: 09 Sep 2022
e-Available: 11 Oct 2022

Keywords

Platooning, Aerodynamics, Lateral offset, Yaw, Cab Over Engine, Drag, CFD, Close Proximity, Intervehicle Distance, Truck, Tractor-Trailer

Citation

Törnell, J., Sebben, S., and Elofsson, P., "Influence of Yaw and Lateral Offset on the Aerodynamics of a Two-Truck Platoon," *SAE Int. J. Commer. Veh.* 16(2):153-164, 2023, doi:10.4271/02-16-02-0010.

ISSN: 1946-391X
e-ISSN: 1946-3928

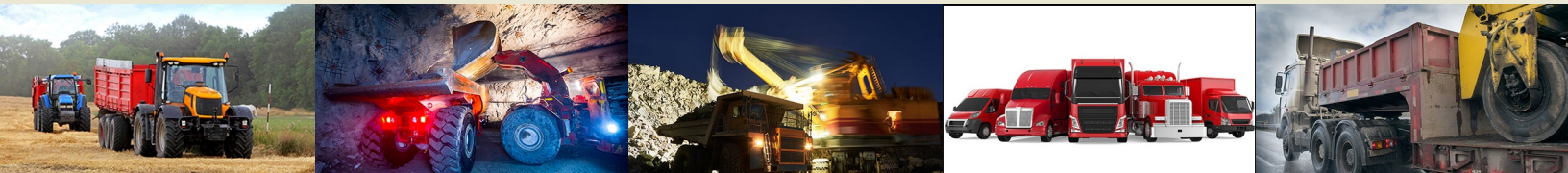

Introduction

Platooning has long been considered a way of reducing the aerodynamic drag of vehicles, thus increasing their energy efficiency. Tougher regulations on greenhouse gas emissions from vehicles, in conjunction with increasing fuel costs and improvements in vehicle automation, have resulted in renewed interest in the concept. The behavior of bodies traveling in close proximity has been studied in several areas, including motorsports, cycling, and trains [1, 2, 3, 4, 5]. Furthermore, some understanding of the behavior at close spacings can be inferred from studies on tractor-trailer gaps in trucks [6, 7]. A large body of research exists on the topic, and different methods have been used with the intent to understand the flow behavior and the aerodynamic gains with platooning. These methods include on-road/track fuel consumption testing, wind-tunnel testing using detailed and simplified models, and numerical simulations.

Studies using North American-style tractor-trailers have shown large improvements in fuel consumption, up to 10% [8, 9, 10, 11, 12]. Similar studies on cab-over-engine-style tractor-trailers (COE) revealed even greater improvements, up to 14% [14, 15, 16, 17]. Many of these investigations showed a continuous decrease in fuel consumption for the leading truck with a decreasing distance between the vehicles. The same holds true for the trailing vehicle with distances greater than 20 m. However, from 20 m to a threshold of around 5 m, the drag goes up, but it goes down again as the distance becomes very short. Further gains with platooning can be obtained with aerodynamic improvements to the trailer of the vehicle, as mentioned in [12, 13]. Studies utilizing the measurement of drag force on a track have investigated the effects of a lateral offset as well as yaw and established that a platoon, in general, has less yaw sensitivity than an isolated vehicle. The studies also confirmed that a lateral offset increases drag if an equal probability of wind direction is assumed and that the drag levels of an in-line platoon and one with a lateral offset in the leeward direction are similar. Moreover, it has been demonstrated that surrounding traffic has a significant impact on the performance of vehicles in a platoon [18].

Wind-tunnel experiments with North American-style tractor-trailer combinations have shown improvements in drag up to large distances as well as the importance of considering the effect of surrounding vehicles when calculating the performance of the combined platoon system. The negative effects on cooling flow have proven to be considerable in these experiments [19, 20, 21, 22]. Studies using simplified bodies report that the shape of the vehicle is of great importance to maximize the efficiency of the system. The preferred shapes for best performance are square backs as the leading vehicle, combined with a square, non-aerodynamic front of the trailing vehicle [23, 24, 25, 26].

Numerical investigations on platooning confirm similar trends to wind-tunnel and on-road tests, except at very short distances where the leading vehicle appears to have lower drag levels than the trailing vehicle. Additionally, the optimal intervehicle distance with respect to drag can also differ between experiments and computations [27, 28, 29, 30, 31]. Several other aspects of platooning have also been investigated numerically. These studies showed an increase in drag for both vehicles when driving alongside each other, with a reduction for the leeward vehicle if it was placed behind the leading vehicle in the next lane [32]. It has also been shown that the front-end radii of the trailing truck can affect the efficiency of a platoon, where greater radii tend to reduce the drag improvements [33]. The performance of platooning has also been compared to an A-train configuration (a tractor with two trailers), and the study confirmed similar drag reductions, however, with a large decrease in cooling flow for the trailing vehicle [34].

Although the available literature is vast, there is still a lack of knowledge on the reasons behind the drag changes at yaw and on the effects of lateral offset for European, cab-over-engine-style tractor-trailers. The aim of this study is to increase the understanding of the flow behavior at short distances under these conditions. The present work uses results from a previous experimental campaign conducted by the authors in the Volvo Cars Aerodynamic wind-tunnel and includes advanced numerical simulations to aid the analysis of the phenomena. The parameters considered are intervehicle distances (IVD) (in full scale) of 0.5, 5, 10, 15, and 20 m; yaw angles of 0, 5, and 10°; and in-line (0 m) and 0.5 m lateral offset.

Method

Test Object

The model used, Figure 1, was a cab-over-engine (COE)-style tractor-trailer combination, which was slightly simplified to ease both simulation and experimental work. The simplifications consisted of a less-detailed engine and gearbox with no cables or tubes in the underhood. Only one of the test models, hereafter termed "the measurement model," had a realistic undercarriage and was equipped with rolling wheels that could be driven by the tunnel belt. This model was kept fixed throughout the tests. The second test object, termed the dummy model, had a simpler underbody of the trailer with a block with semicircles attached to it to represent the wheels and side skirts to reduce the impact of this simplified undercarriage. These differences are not expected to have an impact on the results as the main use of the dummy model was to create a representative blockage in front of or behind the measurement model, depending on its positioning in the platoon. All models had a representation of the cooling system, where the experimental version was built from a honeycomb and mesh combination. The numerical version consisted of three different volumes: a radiator, a charge air cooler, and a combined charge air cooler and condenser for the area in which the condenser covers. The frontal area of the experimental model is 0.28 m^2 and 10 m^2 in the full-scale vehicle CFD model.

FIGURE 1 Model used in this study and location of the pressure taps. The dimensions in 1/6th scale are: A = 2.720 m, B = 0.667 m, C = 0.467 m, D = 2.250, E = 0.625 m, and F = 0.433 m.

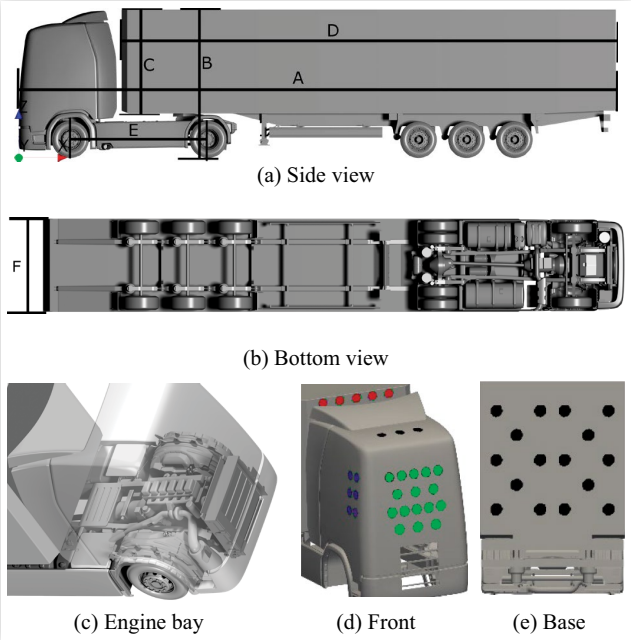

Wind Tunnel

The wind-tunnel used in this study was the Volvo Cars Aerodynamic wind-tunnel, which is of the slotted wall type. The cross-sectional area of the test section is 27.1 m^2, and the slot open ratio is 30%, which yields a blockage ratio of 1.07% with the present models at zero yaw. The tunnel is equipped with a boundary-layer control and ground simulation system consisting of a suction scoop, two perforated ground areas, and five belts with tangential blowers downstream of them. The belts are four-wheel drive units and one center belt, which was used to rotate the wheels of the measurement model in this study. Forces were measured through an under-floor balance with a measurement repeatability of 0.5% of an isolated truck's drag. Forces were averaged over 20 s as is standard in this wind-tunnel; this is equal to 106 flow passages for the longest separation distance of the vehicles. An outline of the test section and the ground simulations system is shown in Figure 2. The light green is the space occupied by the vehicles while varying intervehicle distance, lateral offset, and yaw. The red-filled rectangle is the measurement model fixed at the center belt, and the two outlined blanked rectangles represent the dummy model, which was moved around to create the platoon. With this available space, the dummy model, when in the leading position, could be placed at a maximum 5 m distance (full scale) from the second truck, corresponding to a 0.5 m distance from the start of the test section. At the rearmost position, the dummy model was 1 m from the diffusor.

FIGURE 2 Layout of the ground simulation system and the space used for varying separation distance, lateral offset, and yaw.

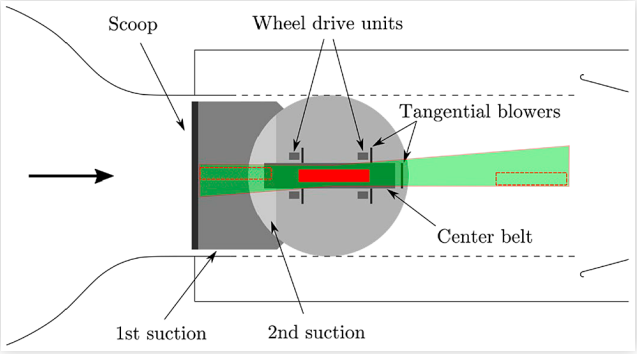

A customized mounting solution, as shown in Figure 3, had to be built for installing the models as the tunnel is designed to test full-scale cars. The mounting of the measurement model, the second one in the figure, consisted of two 6 mm steel cables fastened to the ceiling of the wind-tunnel and four cables to the posts attached to the under-floor balance, allowing for the force measurements. The cables' frontal area is roughly 0.025 m^2, with most of it coming from the two attached to the ceiling. It is expected that half of the drag force exerted on them is experienced by the balance. Although the cables will have an impact on the absolute values, their effect is likely to be small. The drag delta trends

FIGURE 3 Mounting solution: leading truck is the dummy model and trailing truck is the measurement model. Top image is with the beam and bottom without.

should not be influenced. The rolling resistance of the wheels was removed by spinning up the center belt to the correct speed with the wind off and the balance was then tared. This should remain accurate even if the model moves slightly due to lift forces as the wheels are floating and only attached to the truck via a pivot. Mounting of the dummy model was done through four 6 mm steel cables attached to the floor. When positioned over the center belt, a beveled 20 mm tall steel beam was placed underneath to avoid damage to the belt. This should have an impact on the results, which was not considered here, as this was the only viable installation solution. The wind-tunnel boundary-layer control system was run in two different modes based on if the dummy model was placed in front or behind the measurement model. When in front, it stands on the distributed suction system; therefore, the system was turned off not to impact the flow underneath. When behind, the system was on. Neither of the configurations used the tangential blowers to ease comparisons with numerical simulations. At the measurement model position, the boundary-layer thickness is 16 mm when all control systems are on, and when the distributed suction system is turned off the boundary layer grows 20 mm over the distributed suction section. This maximum thickness is about 21% of the model's wheel diameter. This should have a local influence around the wheels and in the lower part of the base wake, but according to Söderblom et al. [37], these local changes should not have much impact on the rest of the wake, nor on drag. All five belts were run at the corresponding wind velocity for all cases.

Numerical Set-Up

Unsteady simulations with the k-w SST IDDES turbulence model were conducted. A second-order implicit time marching scheme was used with a hybrid discretization scheme for convection. A mixed y+ approach was employed to save cells where possible. This was done to ensure that many configurations could be afforded. The domain size was 4 and 10 vehicle lengths upstream and downstream the first and last vehicle, respectively, 40 vehicle widths wide, and 10 vehicle heights in height. This size of the domain was chosen to minimize the effects of boundaries and allow for configurations at yaw. Six levels of volume refinements were used, one set for zero yaw conditions and one for yaw conditions; and the ones for zero yaw are shown in Figure 4. The surface of the vehicle was split into five categories, and different mesh targets were applied to each, Figure 5.

FIGURE 4 Volume mesh refinement boxes at zero yaw. The values correspond to the cell size in mm. For the yaw cases, the 240 mm, 120 mm, and 60 mm refinement boxes were extended to the leeward side by sweeping them around the front corner to 10°.

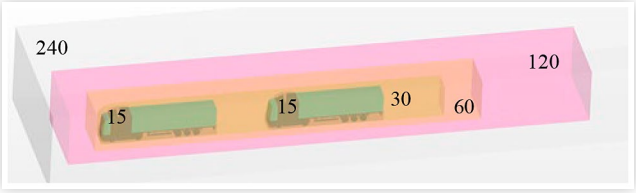

© Johannes Törnell

FIGURE 5 Surface mesh refinement and their respective cell sizes; blue = low $y+$ 7.5 mm, green = high $y+$ 7.5 mm, purple = low $y+$, 15 mm, red = high $y+$ 15 mm, yellow = high $y+$ 30 mm. Low $y+$ corresponds to a $y+$ of 1 and high $y+$ is 30-50.

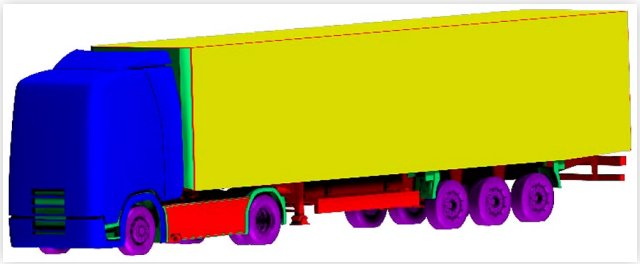

© Johannes Törnell

The time resolution in the simulations was divided into four parts: three of which were used to generate a developed flow and the final was the averaging portion. These steps were 15 s with a time step of 0.1 s, followed by 5 s with a time step of 0.01 s, and 2 s at the final time step size of 0.8 ms. The solution was then averaged over 10 s. The numerical procedure was thoroughly evaluated using many different criteria, such as two-point correlation, turbulent viscosity ratio, and IDDES blending function. The latter is presented in Figure 6. More details of the checks performed to validate the CFD method can be found in [35].

Results

Experimental versus Numerical Results

In this section, the validation of the CFD methodology is demonstrated in terms of a normalized Cd. The normalization is made using corresponding values for a single truck. Note that, as the CFD simulations did not include the full wind-tunnel geometry, we will be looking mostly at validating trends and not absolute values.

As can be seen in Figure 7, the general trends agree well between the numerical and experimental results. There are, however, differences in the deltas between configurations calculated with the two methods. It can be said that the savings for the leading truck are greater in the numerical

FIGURE 6 IDDES blending function: 0 is LES and 1 is URANS.

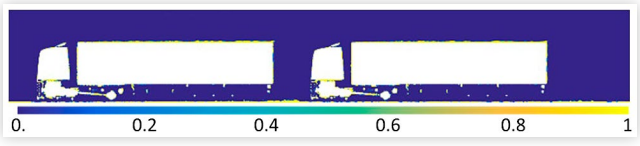

© Johannes Törnell

FIGURE 7 Normalized Cd for both numerical (full lines) and experimental campaigns (dashed lines). The lateral offset (0.5 m) is on the leeward side. Normalization is done toward an isolated truck under corresponding conditions.

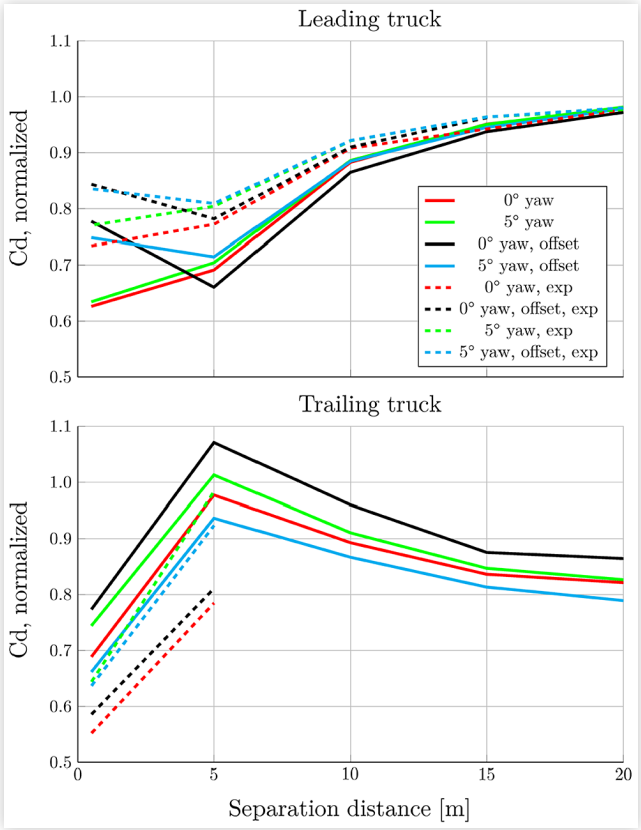

FIGURE 8 Normalized Cd for all numerical simulation cases. Normalization is done toward an isolated truck at corresponding yaw angle.

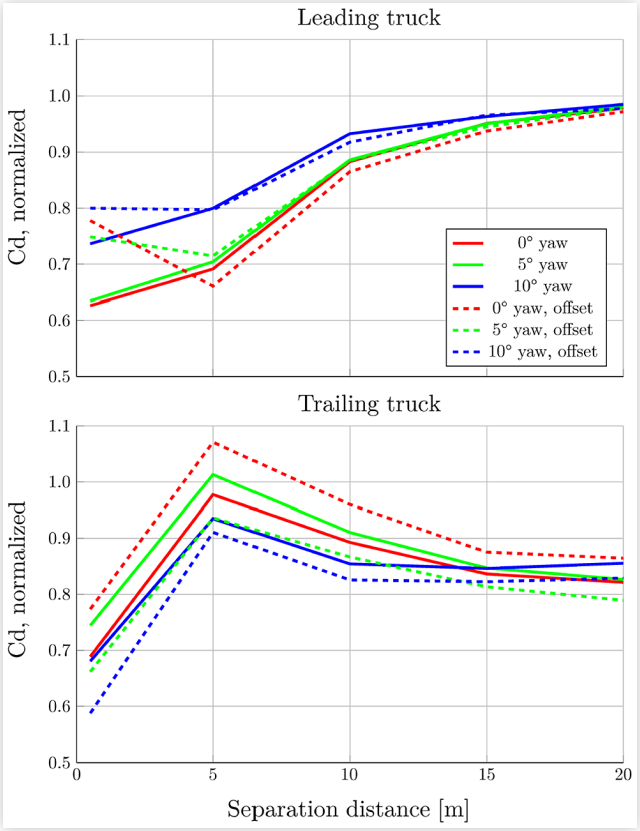

method (lower Cd) than in the tunnel. On the contrary, for the trailing truck, the savings are generally smaller in CFD. As mentioned, part of the discrepancy between the results from the two methods can be attributed to the physical and numerical models not being identical and the complicated installation required in the wind tunnel to keep both trucks in place, something which was not replicated in CFD. With the configuration trends being well captured and with the extensive evaluation of the CFD set-up, the numerical method was deemed to be sufficiently accurate to explore the interactions between the vehicles. As a reminder, the forces for the trailing truck could only be measured for distances up to 5 m as there was limited space upstream in the test section of the wind tunnel.

Drag Reduction Effects Figure 8 shows additional data to Figure 7 and includes results for 10° yaw. The drag for the leading truck is quite insensitive to small yaw angles and offsets at distances greater than 5 m. The drag curve behavior for all angles follows a similar pattern, exhibiting a large increase with a lateral offset at very short distances. The changes in drag observed for the trailing truck are more complex, with a peak in drag at 5 m, which has been reported in many other studies. Furthermore, the changes in normalized drag for a vehicle in a platoon and under yaw conditions are not linear and exhibit an increase in drag with 5° yaw and a decrease with 10° of yaw between 0.5 and 10 m. The increase in drag with 5° yaw is contrary to what has been seen in on-road tests with North American-style trucks. The addition of a lateral offset lowers the drag for all cases with yaw, while with no yaw the drag goes up. This is consistent with what has been seen in other studies but with a larger decrease in drag at yaw. To further understand these effects, we will be looking closely at a few particular cases, using an isolated truck as a comparison.

Isolated Vehicle

The flow around an isolated vehicle is here described in short to ease the understanding of changes in the flow when the truck is in a platoon.

Zero° Yaw At 0° yaw, the time-averaged flow around the truck is symmetrical, see Figure 9, with two counterrotating vortices and low flow velocities underneath the trailer and outside the wheels. The low-pressure regions on the front

FIGURE 9 (a) Coefficient of pressure, (b) and (c) line integral convolution colored by velocity magnitude for an isolated truck at 0° yaw.

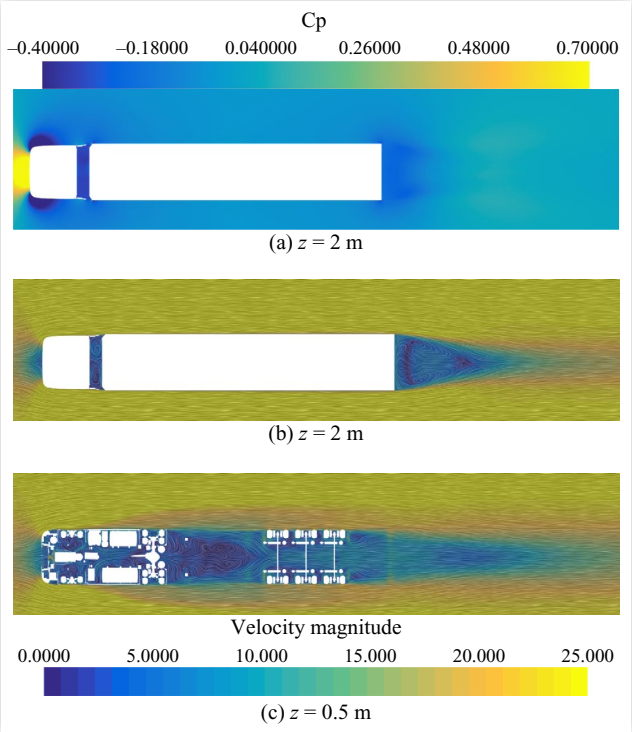

FIGURE 10 (a) Coefficient of pressure, (b) and (c) line integral convolution colored by velocity magnitude for an isolated truck at 5° yaw.

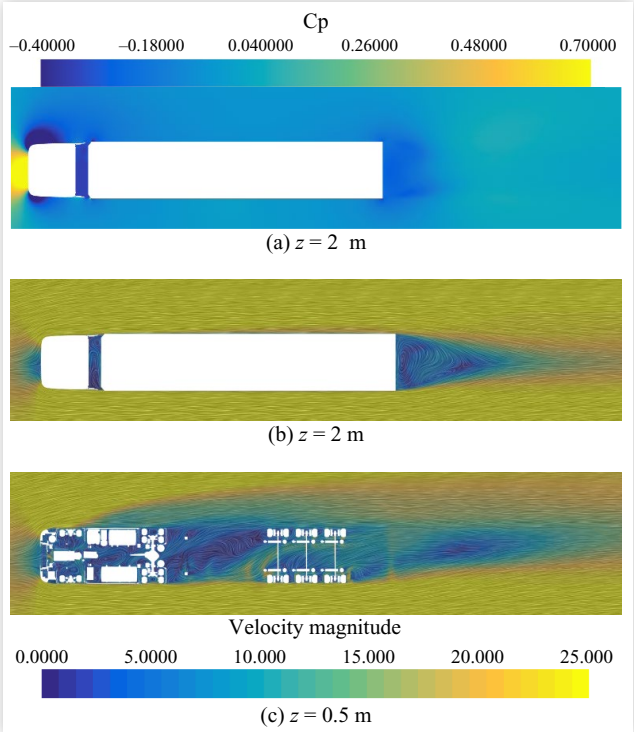

corners of the tractor are also symmetrical, and the stagnation area is centered on the front. The flow underneath the center of the trailer is fed equally by both sides and only with low velocity.

5 and 10° Yaw The addition of yaw induces an asymmetric wake, Figures 10 and 11. Yaw also causes a shift of the stagnation region at the front and an asymmetric acceleration around the tractor corners yielding a larger low-pressure region on the leeward side. In the $z = 0.5$ m plane, there is a cross-flow underneath the trailer and an enlarged separation region from the front wheelhouse. These changes increase the drag from the trailer undercarriage.

Two-Truck Platoon

To analyze the benefits of platooning under the effects of yaw and lateral offset, we define Equation 1, where the drag of the leading or trailing vehicle, $Cd_{Platoon}$, is subtracted by the corresponding values for an isolated truck, $Cd_{isolated}$, at two chosen configurations denoted by subscripts 1 and 2. We term Equation 1 as delta platooning efficiency.

$$\Delta Cd_{Platoon} = \left(Cd_{Platoon} - Cd_{isolated}\right)_1 - \left(Cd_{Platoon} - Cd_{isolated}\right)_2 \quad \text{Eq. (1)}$$

Effects of Yaw In this section, emphasis is placed on the trailing truck as this is the vehicle that experiences the largest influence from yaw.

Leading Truck. As seen in Figure 8, the effects of yaw are small at 5°; therefore, the focus is placed on the 10° yaw case at 5 m intervehicle distance.

Figure 12 shows that the main sources of performance degradation for the leading truck due to yaw are from the trailer undercarriage at the wheels and the base. To further investigate the cause of these changes, the velocity is plotted in Figure 13 at heights $z = 0.5$ and 2 m.

Compared to an isolated vehicle, Figure 11, changes in drag can be traced to differences in the flow underneath the trailer as well as larger asymmetry in the wake. These changes are likely caused by the front of the trailing vehicle entraining the wake by blocking the flow from continuing rearwards, thus forcing it toward the leeward direction and causing an effect similar to that of a larger yaw angle on a single truck. We refer to this effect as an increase in the effective yaw angle, which is particularly visible from the rear half of the leading vehicle, Figures 11(c) and 13(b). The area of lowest velocity of the wake is shifted further to the leeward side yielding higher drag. Flow changes are also observed on the leeward trailer wheels, indicating more lateral flow underneath the vehicle, increasing drag. At 5°,

FIGURE 11 (a) Coefficient of pressure, (b) and (c) line integral convolution colored by velocity magnitude for an isolated truck at 10° yaw.

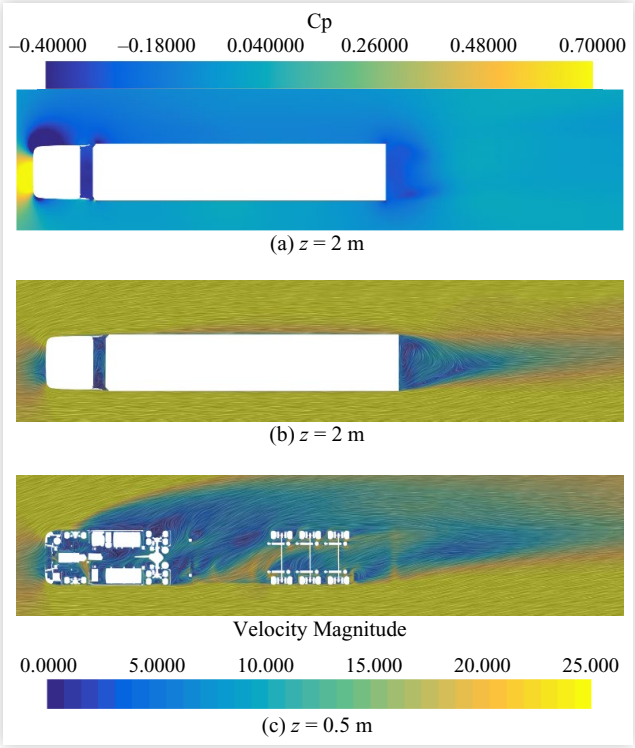

these effects are present but much weaker, yielding smaller or no decrease in platooning performance.

Trailing Truck. The effects of yaw on the trailing truck are more complex than those of the leading vehicle. The delta platooning efficiency along the vehicle is shown in Figure 14 for 5- and 10-° yaw cases at distances of 5 m and 20 m.

Figure 14 shows a loss of efficiency at the front for all cases, with a subsequent improvement over the trailer. The recovery

FIGURE 12 Delta platooning efficiency (Eq. 1) along the leading truck for a platoon with 5 m IVD and zero offset. Configuration 1 is at 10° yaw and Configuration 2 is at 0° yaw. $Cd_{Platoon} = Cd_{Leading\ vehicle}$.

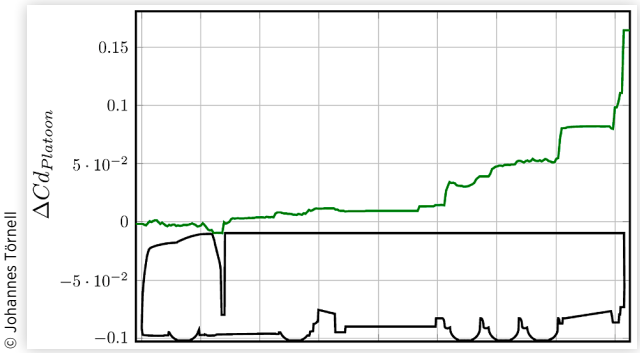

FIGURE 13 Line integral convolution colored by velocity magnitude for the leading vehicle with a separation distance of 5 m at 10° yaw, no lateral offset.

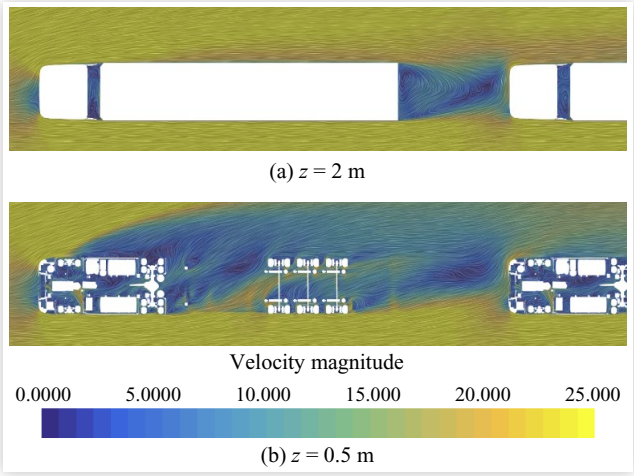

seen for the 5° yaw cases and the 10° yaw at 20 m (green, red, and cyan curves, respectively) is not sufficiently large to compensate for the increase in drag at the front of the vehicle. However, this recovery over the trailer undercarriage is large enough at 10° yaw and 5 m, dark blue curve, causing an improved platooning efficiency.

Additionally, the peak at the front of the trailing truck is higher at 20 m, with a maximum at the very front. To further narrow down the areas of change, so-called X-ray plots are used. These are a way of compressing the distributed drag force on a body to a single plane; here, the *x*-*y* plane is used. This is done by generating a grid of bins where all the drag forces of surface cells of those in-plane bins are summed to one value. These are then plotted to a color gradient to create an easy overview of where the drag is generated on the body.

As can be seen in Figure 15, the changes in drag mostly occur at the front of the vehicle, corners, and tractor-trailer

FIGURE 14 Delta platooning efficiency (Equation 1) along the trailing truck, zero offset. Configuration 1 in the equation is the one seen in the legend and Configuration 2 is the same distance but at 0° yaw.

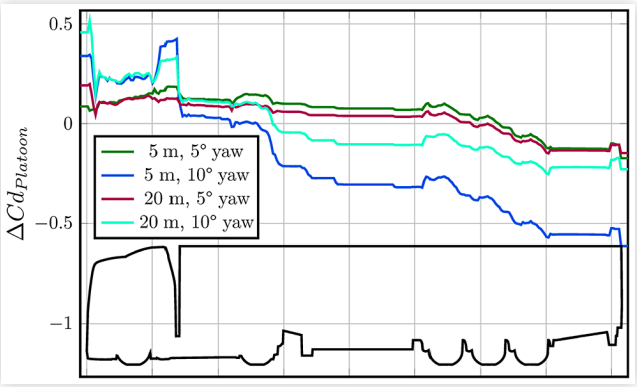

FIGURE 15 X-ray plots created using Equation 1 with $\Delta Cd_{Platoon}$ as the trailing truck. The cases are with no offset, Configuration 2 is 0 yaw, and Configuration 1 is either 5- or 10° yaw (at corresponding IVD). Red indicates an increase in drag; blue indicates a decrease. The colors at the front are saturated and only indicate an area of qualitative increase or decrease.

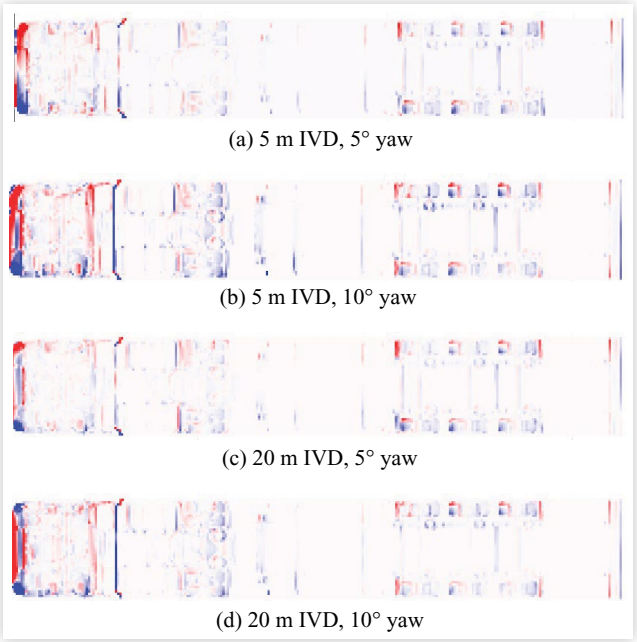

(a) 5 m IVD, 5° yaw

(b) 5 m IVD, 10° yaw

(c) 20 m IVD, 5° yaw

(d) 20 m IVD, 10° yaw

FIGURE 16 Line integral convolution colored by velocity magnitude, trailing truck, no lateral offset.

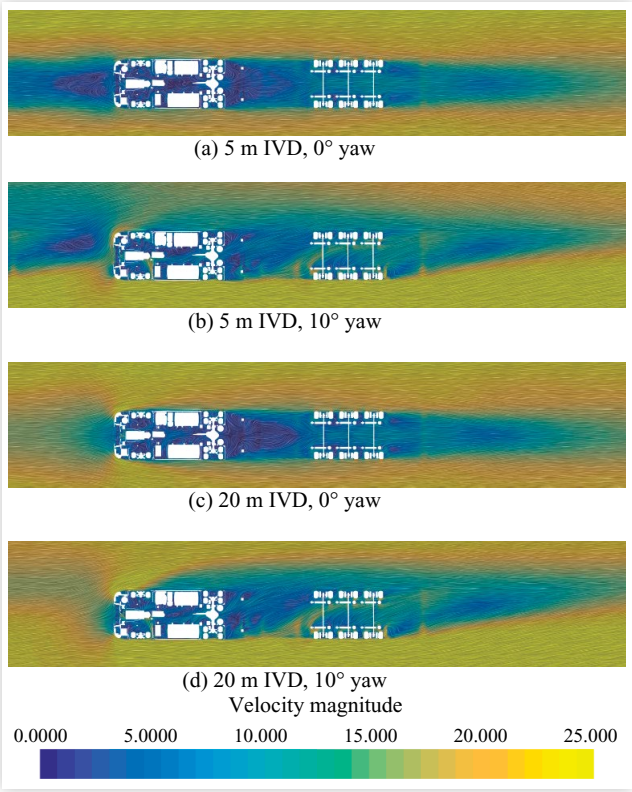

(a) 5 m IVD, 0° yaw

(b) 5 m IVD, 10° yaw

(c) 20 m IVD, 0° yaw

(d) 20 m IVD, 10° yaw

gap (especially for 5 m and the 10° yaw). In general, the leeward side corner sees an increase in drag, with opposite behavior on the windward side. Some changes are also visible on the trailer, but they appear to be more distributed.

With these areas established, the flow field can be investigated to identify which phenomena are the source of these changes. From the plots in Figure 16 and as discussed earlier, the wake of the leading truck is shifted with added yaw, generating a larger stagnation pressure and more acceleration around the corners of the truck. The combination of these two effects is an overall increase in drag. Much of the change over the rest of the vehicle can be attributed to a lower effective yaw angle, caused by the leading truck decreasing the yaw angle as it acts as a blockage forcing the bulk flow to turn locally. This can be seen in the flow underneath the trailer for the two different distances, where there is significantly less cross-flow underneath the trailer for both cases when compared to the isolated vehicle, Figure 11. The reason for the decrease in performance at 20 m vs. 5 m at 10° yaw is that the effects on the front of the trailer become stronger with larger separation distances as the wake of the leading vehicle gets pushed further downwind. Furthermore, the effects of reduced effective yaw angle also grow weaker with a longer distance since this effect is local. This change in dominant effect occurs at roughly 10-15 m.

Effects of Lateral Offset

As presented, yaw causes a shift of the wake leading to higher drag on the front of the trailing truck. In [36] and in Figure 8, it was demonstrated that a possible way of mitigating this negative effect is to position the trailing truck with a lateral offset toward the leeward direction. The benefits are particularly visible at short distances. For the leading truck the effects are small, except at 0.5 m. Simulations with a 0.5 m lateral offset in the leeward direction were run for all cases, and the results are discussed subsequently.

Leading Truck. From the simulations, it could be established that the reason for the drag increase for the leading vehicle at 0.5 m with a 0.5 m lateral offset is a lower base pressure created by a large vortex formed between the two vehicles, starting at the right lower corner (same side of the direction of the offset) (Figure 17). The same was observed in the experimental campaign [36]. This vortex follows the base of the leading truck diagonally and exits on the left side (opposite side of the offset).

This vortex is formed due to the increased lateral and vertical flow between the vehicles. The lateral flow is caused by a stagnation region formed at the front of the trailing vehicle on the exposed side, and the vertical flow is caused by the high ground clearance of the leading trailer in

FIGURE 17 Streamlines colored by Cp seeded along the bottom side edge of the leading truck showing a large vortex formation. Zero yaw, 0.5 m separation distance, and 0.5 m lateral offset.

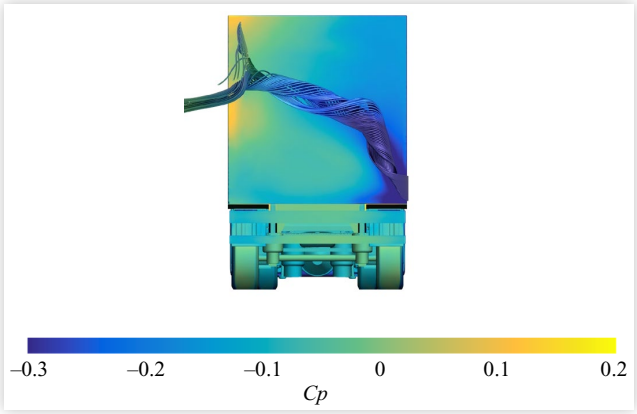

combination with the low ground clearance and rake of the trailing tractor, forcing the air upward.

Trailing Truck. Figure 18 shows that the increase in drag seen when no yaw is present mainly stems from changes at the front of the vehicle and the base of the vehicle. At yaw, the curve behaves quite similarly, except for reversed effects for the front of the tractor, shifting of the stagnation area toward the center and a lowering of the pressure, Figure 20.

The main difference between the zero yaw and the yaw case is that the red area (added drag) is smaller and weaker at the front of the tractor, yielding a lowering of drag for the case at yaw, Figure 19. It can also be seen that the effects on the base are reversed, as seen in Figure 18.

For the case without yaw, a lateral offset corresponds to the trailing truck being positioned toward the edge of the leading truck wake, thus increasing stagnation pressure on the more exposed side of the vehicle, Figure 20. Under yaw

FIGURE 18 Delta platooning efficiency (Equation 1) along the trailing truck, 10 m distance. Configuration 1 is with 0.5 m lateral offset, and Configuration 2 is without offset.

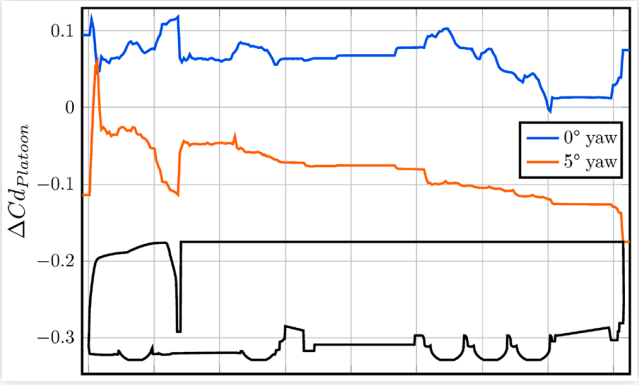

FIGURE 19 X-ray plots created using Equation 1 with $Cd_{Platoon}$ as the trailing truck. The cases are with 10 m separation distance. Red indicates an increase in drag with added lateral offset; blue indicates a decrease. Configuration 1 is with 0.5 m lateral offset, and Configuration 2 without offset.

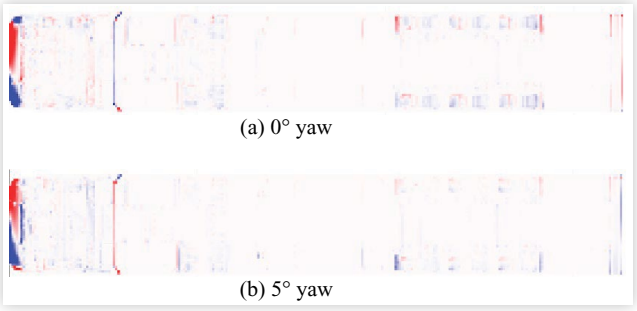

conditions, the vehicle is instead located more at the center of the wake, which contributes to a reduced stagnation pressure. The consequent drag reduction is further reinforced by the decrease in effective yaw angle. This is confirmed from the flow underneath the vehicle being less angled than in the no offset case and with a larger area of low velocity between the trailer axles and rear wheels of the tractor.

Drag of the Combined System

The drag for the combined system, Figure 21, remains fairly constant at distances between 10 and 20 m, with the negative effects of yaw being relatively small. For distances shorter than 10 m, the presence of yaw deteriorates the performance of the platoon, but this can be partially compensated with a lateral offset of the trailing truck. The figure also shows that short distances are essential for maximizing the benefit of platooning and that for the very shortest one (0.5 m), no lateral offset is the most beneficial position, except for at 10° yaw. Although 10° yaw is not a

FIGURE 20 Line integral convolution colored by velocity magnitude, trailing truck 0.5 m lateral offset.

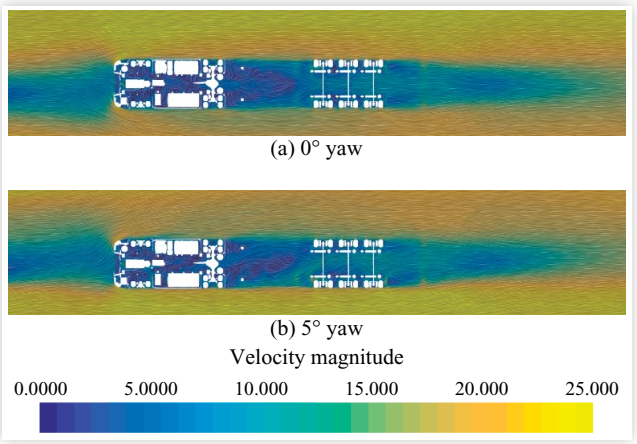

FIGURE 21 Combined normalized drag for the two trucks vs. separation distance. The normalized drag for the entire platoon is $Cd_{normalized} = (Cd_{Leading} + Cd_{Trailing})/(2 * Cd_{Isolated})$.

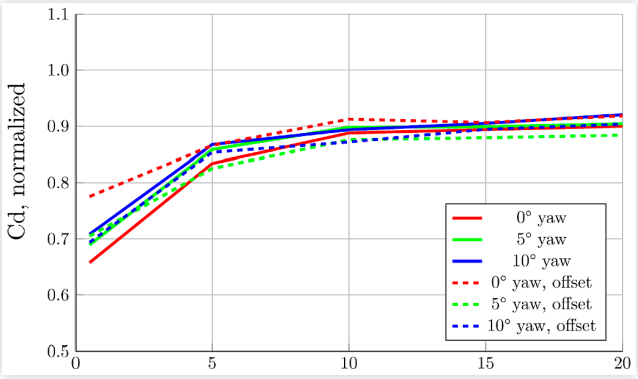

very frequent occurrence, it is still important to understand the potential decrease in efficiency.

Conclusions

The aerodynamic behavior of COE tractor-trailer combinations traveling in close proximity was studied numerically, considering the effects of yaw and lateral offset at several intervehicle distances. The results show that different effects are responsible for the positive gains of platooning in the conditions investigated. For the leading truck, most effects are observed in the base pressure. The truck sees only minor changes when a lateral offset is added, except at very short intervehicle distances. At a short distance, a strong vortex is formed in the gap between the two vehicles, lowering the base pressure and greatly increasing drag for the leading vehicle. Regarding yaw, the negative effects are more prominent at short intervehicle distances and with angles larger than 5°. In general, the trailing truck experiences an improved relative performance at large yaw angles and a degraded performance at small yaw angles. This is due to the balance between two effects, namely, the front of the vehicle being further away from the center of the leading vehicle's wake, increasing drag, and the effective yaw angle being reduced due to the leading vehicle, reducing drag. These two effects also cause changes in drag when a lateral offset is applied under yaw conditions, with both effects reducing drag as the vehicle is moved back into the wake. The drag for the combined system is fairly constant between 10 to 20 m. For distances shorter than 10 m, the presence of yaw deteriorates the performance of the platoon, which can be partially compensated with an offset of the trailing truck. Finally, as the distribution of drag reduction varies greatly between the two vehicles with different conditions, more studies are necessary to better understand the phenomena and the savings involved.

Further areas of interest involve the behavior of multiple vehicle types, more than two vehicles in the platoon, and the effects of typical drag reduction devices on the platooning of COE-style tractor-trailers.

Acknowledgment

The computations were enabled by resources provided by the Swedish National Infrastructure for Computing at NSC partially funded by the Swedish Research Council through grant agreement no. 2018-05973.

Contact Information

Johannes Törnell
Johannes.tornell@chalmers.se
+46702797776

References

1. Blocken, B., Toparlar, Y., van Druenen, T., and Andrianne, T., "Aerodynamic Drag in Cycling Team Time Trials," *J. Wind Eng. Ind. Aerod.* 182 (2018): 128-145.
2. Blocken, B., van Druenen, T., Toparlar, Y., Malizia, F. et al., "Aerodynamic Drag in Cycling Pelotons: New Insights by CFD Simulation and Wind Tunnel Testing," *J. Wind Eng. Ind. Aerod.* 179 (2018): 319-337.
3. Jacuzzi, E. and Granlund, K., "Passive Flow Control for Drag Reduction in Vehicle Platoons," *J. Wind Eng. Ind. Aerod.* 189 (2019): 104-117.
4. Li, C., Burton, D., Kost, M., Sheridan, J. et al., "Flow Topology of a Container Train Wagon Subjected to Varying Local Loading Configurations," *J. Wind Eng. Ind. Aerod.* 169 (2017): 12-29.
5. Maleki, S., Burton, D., and Thompson, M.C., "Flow Structure between Freight Train Containers with Implications for Aerodynamic Drag," *J. Wind Eng. Ind. Aerod.* 188 (2019): 194-206.
6. Allan, J., "Aerodynamic Drag and Pressure Measurements on a Simplified Tractor-Trailer Model," *J. Wind Eng. Ind. Aerod.* 9, no. 1 (1981): 125-136.
7. Östh, J. and Krajnovic, S., "The Flow around a Simplified Tractor-Trailer Model Studied by Large Eddy Simulation," *J. Wind Eng. Ind. Aerod.* 102 (2012): 36-47.
8. Lammert, M.P., Duran, A., Diez, J., Burton, K. et al., "Effect of Platooning on Fuel Consumption of Class 8 VEHICLES over a Range of Speeds, Following Distances, and Mass," *SAE Int. J. Commercial Vehicles* 7, no. 2 (2014): 626-639, doi:https://doi.org/10.4271/2014-01-2438.
9. Lammert, M.P., Kelly, K.J., and Yanowitz, J., *Correlations of Platooning Track Test and Wind Tunnel Data* (Golden, CO: National Renewable Energy Laboratory, 2017)

10. Al Alam, A., Gattami A., and Johansson, K.H., "An Experimental Study on the Fuel Reduction Potential of Heavy Duty Vehicle Platooning," in *13th International IEEE Conference on Intelligent Transportation Systems*, Funchal, Portugal, 2010.
11. Browand, F., McArthur, J., and Radovich, C., "Fuel Saving Achieved in the Field Test of Two Tandem Trucks," California PATH Research Report UCB-ITS-PRR-2004-20, 2004.
12. McAuliffe, B., Croken, M., Ahmadi-Baloutaki, M., and Raeesi, A., "Fuel-Economy Testing of a Three-Vehicle Truck Platooning System," Technical Report LTR-AL-2017-0008, National Research Council Canada, 2017.
13. McAuliffe, B., Lammert, M., Lu, X.Y., Shladover, S. et al., "Influences on Energy Savings of Heavy Trucks Using Cooperative Adaptive Cruise Control," SAE Technical Paper 2018-01-1181, 2018, https://doi.org/10.4271/2018-01-1181.
14. Bonnet, C. and Fritz, H., "Fuel Consumption Education in a Platoon: Experimental Results with Two Electronically Coupled Trucks at Close Spacing," SAE Technical Paper 2000-01-3056, 2000, https://doi.org/10.4271/2000-01-3056.
15. Davila, A., Aramburu, E., and Freixas, A., "Making the Best Out of Aerodynamics: Platoons," SAE Technical Paper 2013-01-0767, 2013, https://doi.org/10.4271/2014-01-2438.
16. Tsugawa, S., "Results and Issues of an Automated Truck Platoon within the Energy ITS Project," in *IEEE Intelligent Vehicles Symposium Proceedings*, 2014, 642-647.
17. Tsugawa, S., Kato, S., and Aoki, K., "An Automated Truck Platoon for Energy Saving," in *IEEE/RSJ International Conference on Intelligent Robots and Systems*, San Francisco, CA, 2011.
18. McAuliffe, B., Smith, P., Raeesi, A., Hoffman, M. et al., "Track-Based Aerodynamic Testing of a Two-Truck Platoon," *SAE Int. J. Adv. & Curr. Prac. in Mobility* 3, no. 3 (2021): 1450-1472, doi:https://doi.org/10.4271/2021-01-0941.
19. Hammache, M., Michaelian, M., and Browand, F., "Aerodynamic Forces on Truck Models, Including Two Trucks in Tandem," SAE Technical Paper 2002-01-0530, 2002, https://doi.org/10.4271/2002-01-0530.
20. Salari, K. and Ortega, J., "Experimental Investigation of the Aerodynamic Benefits of Truck Platooning," SAE Technical Paper 2018-01-0732, 2018, https://doi.org/10.4271/2018-01-0732.
21. McAuliffe, B. and Ahmadi-Baloutaki, M., "A Windtunnel Investigation of the Influence of Separation Distance, Lateral Stagger, and Trailer Configuration on the Drag-Reduction Potential of a Two-Truck Platoon," *SAE Int. J. Commer. Veh.* 11, no. 2 (2018): 125-150, doi:https://doi.org/10.4271/02-11-02-0011.
22. McAuliffe, B. and Ahmadi-Baloutaki, M., "An Investigation of the Influence of Close-Proximity Traffic on the Aerodynamic Drag Experienced by Tractor-Trailer Combinations," SAE Technical Paper 2019-01-0648, 2019, https://doi.org/10.4271/2019-01-0648.
23. Schito, P. and Braghin, F., "Numerical and Experimental Investigation on Vehicles in Platoon," *SAE Int. J. Commer. Veh.* 5, no. 1 (2012): 63-71, doi:https://doi.org/10.4271/2012-01-0175.
24. Le Good, G., Resnick, M., Boardman, P., and Clough, B., "Effects on the Aerodynamic Characteristics of Vehicles in Longitudinal Proximity due to Changes in Style," SAE Technical Paper 2018-37-0018, 2018, https://doi.org/10.4271/2018-37-0018.
25. Fletcher, C. and Stewart, G., "Bus Drag Reduction by the Trapped Vortex Concept for a Single Bus and Two Buses in Tandem," *J. Wind Eng. Ind. Aerod.* 24, no. 2 (1986): 143-168.
26. Watkins, S. and Vino, G., "The Effect of Vehicle Spacing on the Aerodynamics of a Representative Car Shape," *J. Wind Eng. Ind. Aerod.* 96, no. 6 (2008): 1232-1239, *5th International Colloquium on Bluff Body Aerodynamics and Applications*.
27. Humphreys, H. and Bevly, D., "Computational Fluid Dynamic Analysis of a Generic 2 Truck Platoon," SAE Technical Paper 2016-01-8008, 2016, https://doi.org/10.4271/2016-01-8008.
28. Humphreys, H., Batterson, J., Bevly, D., and Schubert, R., "An Evaluation of the Fuel Economy Benefits of a Driver Assistive Truck Platooning Prototype Using Simulation," SAE Technical Paper 2016-01-0167, 2016, https://doi.org/10.4271/2016-01-0167.
29. Smith, J., Mihelic, R., Gifford, B., and Ellis, M., "Aerodynamic Impact of Tractor-Trailer in Drafting Configuration," *SAE Int. J. Commer. Veh.* 7, no. 2 (2014): 619-625, doi:https://doi.org/10.4271/2014-01-2436.
30. Ellis, M., Gargoloff, J., and Sengupta, R., "Aerodynamic Drag and Engine Cooling Effects on Class 8 Trucks in Platooning Configurations," *SAE Int. J. Commer. Veh.* 8, no. 2 (2015): 732-739, doi:https://doi.org/10.4271/2015-01-2896.
31. Bevly, D., Murray, C., Lim, A., Turochy, R. et al., "Heavy Truck Cooperative Adaptive Cruise Control: Evaluation, Testing, and Stakeholder Engagement for Near Term Deployment: Phase Two," Final Technical Report, Auburn University, 2017.
32. Vegendla, P., Sofu, T., Saha, R., Kumar, M. et al., "Investigation of Aerodynamic Influence on Truck Platooning," SAE Technical Paper 2015-01-2895, 2015, https://doi.org/10.4271/2015-01-2895.
33. Gheyssens, T. and Van Raemdonck, G., "Effect of the Frontal Edge Radius in a Platoon of Bluff Bodies," *SAE Int. J. Commer. Veh.* 9, no. 2 (2016): 371-380, doi:https://doi.org/10.4271/2016-01-8149.
34. Mihelic, R., Smith, J., and Ellis, M., "Aerodynamic Comparison of Tractor-Trailer Platooning and A-Train Configuration," *SAE Int. J. Commer. Veh.* 8, no. 2 (2015): 740-746, doi:https://doi.org/10.4271/2015-01-2897.
35. Törnell, J., Sebben, S., and Söderblom, D., "Influence of Inter-Vehicle Distance on the Aerodynamics of a Two-Truck Platoon," *Int. J Automot. Technol.* 22 (2021): 747-760, doi:https://doi.org/10.1007/s12239-021-0068-5.

36. Törnell, J., Sebben, S., and Elofsson, P., "Experimental Investigation of a Two-Truck Platoon Considering Inter-Vehicle Distance, Lateral Offset and Yaw," *Journal of Wind Engineering and Industrial Aerodynamics* 213 (2021): 104596, http://doi.org/10.1016/j.jweia.2021.104596.

37. Söderblom, D., Löfdahl, L., Elofsson, P., and Hjelm, L., "An Investigation of the Aerodynamic Drag Mechanisms due to Ground Simulation in Yawed Flow Conditions for Heavy Trucks", in *ASME 2009 Fluids Engineering Division Summer Meeting*, Vail, CO, 2009, FEDSM2009-78519.